Proc. of the Intl. Conf. on Advances In Bio-Informatics,Bio-Technology And Environmental Engineering-ABBE 2014.

ISBN: 978-1-63248-009-5 doi: 10.15224/ 978-1-63248-009-5-87

Comparison of surface reflectance values from the USGS Landsat 5 TM climate data record (CDR) with values generated using a simple dark object subtraction (DOS) method in an Alpine watershed

P.S. Sawyer and H. Stephen

***Abstract*— Extraction of relevant information from remotely sensed imagery is essential for the identification of changes in the earth's environment. Methods for converting the data collected at the sensor to surface reflectance have been under constant improvement since the beginning of the Landsat program. The time and effort needed to perform this task has recently been eliminated with the publication of the USGS Landsat CDR. This paper compares the data available from the USGS with a simple dark object subtraction method for determining surface reflectance. Our goal is to determine if the USGS data set is comparable to previous methods. We find that the USGS data set is strongly correlated with the simpler DOS method. While clear differences in absolute surface reflectance are observed in the visible and near-IR bands, the trends in the data over time are consistent. This suggests that previous trend studies using the simpler methods do not need to be revisited using the newer data. The findings also suggest that researchers no longer need to perform the labor intensive step of converting raw data to surface reflectance by making use of the USGS surface reflectance data instead.**

***Keywords*— Landsat, Thematic Mapper, USGS Climate Data Record, remote sensing, Alpine watershed, climate change, time series Mann-Kendall trend analysis**

I. Introduction

Understanding changes in Earth's environment is becoming ever more critical as the pace of those changes increases due to factors including anthropogenic influence on global mass and energy balances.

Patrick Sawyer
University of Nevada, Las Vegas
United States

Haroon Stephen, PhD
University of Nevada, Las Vegas
United States

Spaceborne instruments, that can effectively monitor the biosphere, have become essential tools to enhance our ability to adapt to future environmental conditions brought about by complex processes such as climate change and population growth (Chung et al., 2010). The Landsat program has been indispensable in the analysis of temporal changes in the environment. Landsat earth observation sensors have been in continuous orbit since 1972, providing an unparalleled opportunity to observe changes to the environment and to develop analytical techniques that can relate the Landsat remote sensing data to natural and anthropogenic processes responsible for the observed changes. Examples of how this data is applied to ecological science include: analysis of net primary productivity (NPP) and species richness; monitoring of climate variables such as temperature, precipitation, and soil moisture; determining species distributions and habitat structure including topography (Turner et al., 2003).

The ecological response to elevated temperatures and CO_2 levels is complex and will be affected by many factors including water and other nutrient resource availability. In cold alpine regions where water availability is not limiting, higher temperatures are expected to increase the habitable zones for several species, allowing for upslope migration and increased vegetative cover. Higher temperatures combined with increased atmospheric CO_2 levels will increase photosynthesis resulting in increased biomass; provided other essential resources are not limited (Skre and Naess, 1999). Conversely, where water is limited, higher temperatures will increase plant stress resulting in reduced vegetative cover (Chmura et al., 2011).

In order to use the wealth of information contained in the Landsat archive database, methods for converting the raw digital numbers recorded by the sensor to actual surface reflectance must be used. The common methodology for this conversion is to first convert the digital numbers to the at sensor radiance value, followed by conversion to Top-of-Atmosphere (TOA) reflectance and finally applying an atmospheric correction to determine the surface reflectance.

There are many atmospheric correction procedures that have been developed over the last three decades, and with the addition of atmospheric profiling remote sensors, many atmospheric correction algorithms are now available that include actual upwelling and downwelling radiance values in the analysis. However, in order to take advantage of the older

Proc. of the Intl. Conf. on Advances In Bio-Informatics,Bio-Technology And Environmental Engineering-ABBE 2014.

ISBN: 978-1-63248-009-5 doi: 10.15224/ 978-1-63248-009-5-87

Landsat imagery (< 2000), other methods, typically imaged based, are used. One of the most common atmospheric correction methods is known as "Dark Object Subtraction or DOS". This method is based on the assumption that radiance seen at the satellite for "dark" pixels (i.e. deep water) result purely from atmospheric path radiance. A derivation of the DOS technique known as the Cos θ or "COST" method is used in this analysis due to its simplicity and ease of use. This method assumes that even dark objects will possess some reflectance, so a value of 1% is assigned to the dark object to more accurately reflect actual surface reflectance (Chavez, 1996).

The determination of surface reflectance from the raw Landsat data can be a time consuming and complicated procedure. Fortunately, the United State Geological Survey (USGS) has automated this task and published a complete set of surface reflectance data derived from raw Landsat 5 Thematic Mapper TM and Landsat 7 Enhanced Thematic Mapper (ETM+) imagery. The data, designated the Climate Data Record (CDR), is available from the USGS EarthExplorer (http://earthexplorer.usgs.gov/) website. The CDR data set was developed under the Landsat Ecosystem Disturbance Adaptive Processing System (LEDAPS) program. The LEDAPS project made use of the existing MODIS Adaptive Processing System (MODAPS) developed for the Moderate Resolution Imaging Spectroradiometer (MODIS) sensor to convert raw at-sensor data to surface reflectance (Masek et al., 2006).

While the availability of this data will no doubt enhance the standardization and utilization of the Landsat data archive, it is important to consider how this data set differs from the surface reflectance values determined in previous studies. This information will allow us to evaluate the usefulness of revisiting those previous studies to determine if their findings may be altered by use of this new data set.

In this study, we compare the surface reflectance data generated by the USGS with the surface reflectance generated using a simple Dark Object Subtraction atmospheric correction based on the COST algorithm developed by Chavez, 1996. The two data sets are compared using simple linear regression. Correlation coefficients are determined for each data set for each of the six reflective bands of the Landsat 5 TM sensor. We analyze the data in several ways included a simple comparison of all data sets and how those comparisons have trended over time. We also compare the data sets based on land class, elevation, and vegetative density to determine which parameters may show significant disagreement. The study area is an ecologically sensitive Alpine watershed in California's Eastern Sierra Nevada Mountains.

II. Study Area and Data

A. *Study Area Description*

Fig. 1 below shows the Big Pine Creek watershed located in California's Eastern Sierra Mountains. Big Pine Creek is a major tributary to the Owens River which is a significant source of fresh water for Los Angeles.

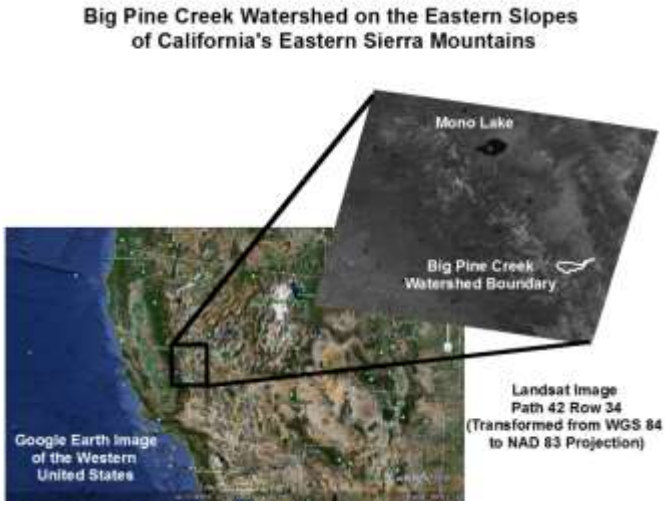

Figure 1: Study area location showing the boundary of the Big Pine Creek watershed.

The Owens River valley straddles the Great Basin and Mojave deserts with vegetation consisting primarily of pine forests at higher elevations and xeric species at lower elevations. Areas bordering streams and the Owens River are primarily grass dominated meadows (Elmore et al., 2003). Elevation within the watershed increases from East to West with the higher regions dominated by barren rock and woodlands with the lower regions dominated by mixed desert shrubs.

The Big Pine Creek watershed ecosystem owes its existence to snow melt and melt-water from the Palisade Glacier. In addition to being the southern-most glacier in the United States, it is also the largest glacier in the Sierras with a surface area of 1.3 km^2. It was formed about 3,200 years ago, reaching a maximum extent as recently as 170 years ago (Bowerman and Clark, 2011). It has been generally in retreat ever since. The Big Pine Creek watershed drainage area covers approximately 82 km^2 and its average flow is 1.8 m^3/s. Measurements taken in the 1980's indicate that the creek is a gaining stream at the lower elevations in contrast to most other Owens River tributaries which are losing streams (Kondolf, 1989). Since all of the living species within this watershed depend on the glacier and snow melt for their survival, the impact of temperature and precipitation variations on the biodiversity of the Big Pine Creek watershed can serve as a predictor of how other ecologically sensitive and critically essential watersheds will respond to future climate regimes.

There are 34 land cover classifications in the Big Pine Creek watershed with the ten most abundant covering 93% of the total surface area. These top ten land cover classifications are listed in table 1 along with their relative abundance. The USGS provides land cover information to the public through an online mapping service from the University of Idaho (http://www.gap.uidaho.edu/landcoverviewer.html). In order to ensure a representative sample of numerous vegetative species present in the watershed, three sample sites at different elevations, from each of the ten most abundant land cover classifications are selected for a total of 30 sample sites.

Proc. of the Intl. Conf. on Advances In Bio-Informatics,Bio-Technology And Environmental Engineering-ABBE 2014.

ISBN: 978-1-63248-009-5 doi: 10.15224/ 978-1-63248-009-5-87

TABLE 1: Land Cover Classifications in the Big Pine Creek Watershed

USGS Land Class Level 3	Land Type	Class ID	PIXEL COUNT	% of Pixels
Mediterranean California Alpine Bedrock and Scree	Barren (B2)	3504	46547	39.16
Great Basin Pinyon-Juniper Woodland	Woodland (W2)	4514	25196	21.19
Inter-Mountain Basins Montane Sagebrush	Shrub (S2)	5308	10597	8.91
Inter-Mountain Basins Big Sagebrush Shrubland	Shrub (S3)	5706	9925	8.35
Sierra Nevada Subalpine Pine Forest and Woodland	Woodland (W3)	4533	6819	5.73
Sierra Nevada Cliff and Canyon	Barren (B1)	3215	2857	2.40
Inter-Mountain Basins Mixed Salt Desert Scrub	Shrub (S1)	5205	2827	2.37
Developed, Open Space	Developed (D1)	1201	1966	1.65
Mediterranean California Red Fir Forest	Woodland (W1)	4318	1872	1.57
Northern California Mesic Subalpine Woodland	Woodland (W4)	4608	1585	1.33

These ten land cover classes fall into four types, barren, woodland, shrub, and developed. Differences in how the various land types have responded to climate change will provide insight into which ecological processes are being most affected by recent variation in environmental parameters.

In addition to the 30 sites selected by land class, three sites were selected for every 100 meter elevation gradient from 1200 meters MSL to 3600 meters MSL. At each gradient, a densely vegetated site, a moderately vegetated site, and a sparsely vegetated site were selected. These 75 sample sites based on elevation gradient and vegetative density combined with the 30 sites chosen by land class provide a total of 105 sample sites that will be analyzed for comparison between the USGS CDR surface reflectance and the simplified DOS determined surface reflectance.

B. Data

The Landsat program has been providing earth observation remote sensing data to the scientific community for four decades. The first Landsat satellite was placed in orbit in 1972 with Landsat 7 remaining operational today. Landsat 5 was only recently taken off-line. The next generation satellite, the Landsat Data Continuity Mission (Landsat 8), was launched on February 11th, 2013 is now operational. Unfortunately, the Landsat 7 ETM+ imager suffered a scan line correction malfunction in 2003 that causes significant striping across the study area, making data acquired since that event difficult to use. In this analysis, we use only Landsat 5 TM data collected over a 28 year period from 1984 through 2011. Using a single sensor ensures maximum consistency of the data and eliminates errors associated with correlating data from multiple sensors.

Table 2 details the six reflective bands of the TM sensor, covering the blue, green, red, near infrared (NIR), short-wave infrared (SWIR), and mid-wave infrared (MWIR) regions of the spectrum as well as their ecological applications.

TABLE 2: Landsat 5 TM Band Description and Ecological Application

Band	Spectral Range (μm)	Resolution (m)	Region	Common Applications
1	0.45-0.52	30	Blue	Soil/Vegetation
2	0.52-0.60	30	Green	Vegetation Vigor
3	0.63-0.69	30	Red	Chlorophyll
4	0.76-0.90	30	NIR	Biomass Surveys
5	1.55-1.75	30	SWIR	Vegetation/Soil
6	10.4-12.5	120	TIR	Soil Moisture
7	2.08-2.35	30	MWIR	Hydrothermal

Bands 5 and 7 are sometimes referred to as SWIR1 and SWIR2. However, in this study, we refer to band 5 as the SWIR and band 7 as the MWIR. Band 6 covers the thermal infrared (TIR) and the data from this region is not used in this study. These descriptions are retrieved from the Northern Arizona University Infrared Spectrometry Laboratory website (http://www.cefns.nau.edu/seses/llecb/Spectrometer/RemoteSensing.html).

DOS Data

The Landsat 5 TM imagery used in this analysis was acquired for 28 dates in the month of July from 1984 (year of launch) through 2011 (year turned off). Most of the imagery used in this analysis is from Path 42, Row 34 with four of the images from Path 41, Row 34. Both image ID ground swaths cover the entire study area. The Landsat imagery used in this analysis are listed in table 3 below. Since the period of maximum leaf area index generally occurs in the mid-June to mid-August time frame (Gond et al., 1999), only imagery in the July time frame was considered for this analysis in order to minimize the impacts of the phenological cycle on the reflectance data.

The imagery used to develop the DOS set consisted of GeoTIFF formatted georeferenced and radiometric corrected files that were processed using ArcMap v 10.1 to produce the raw digital numbers recorded by the sensor over each sample point. Each of the bands from the GeoTIFF file was added as a layer to the ArcMap file which allows for identification of each Digital Number for each band for all 105 sample sites recorded by the sensor on that date.

USGS CDR

The CDR data set consisted of the same imagery with the raw digital numbers replaced by calculated surface reflectance values for each of the six reflective bands of the Landsat 5 TM sensor. USGS surface reflectance data is generated from a software package known as the Landsat Ecosystem Disturbance Adaptive Processing System (LEDAPS). The surface reflectance data is generated by applying an atmospheric correction to the raw Landsat 5 TM imagery (USGS, 2013).

This atmospheric correction uses the Second Simulation of a Satellite Signal in the Solar Spectrum (6S) radiative transfer model to account for various atmospheric column constituents including water vapor, ozone, and aerosol optical thickness (Masek et al., 2006).

Proc. of the Intl. Conf. on Advances In Bio-Informatics,Bio-Technology And Environmental Engineering-ABBE 2014.

ISBN: 978-1-63248-009-5 doi: 10.15224/ 978-1-63248-009-5-87

TABLE 3: Summary of Landsat imagery used in this analysis

Image Date	Time	Scene ID (Path/Row)	Image Date	Time	Scene ID (Path/Row)
7/18/2011	10:22	42/34	7/27/1997	10:04	42/34
7/31/2010	10:24	42/34	7/8/1996	9:47	42/34
7/5/2009	10:16	41/34	7/22/1995	9:38	42/34
7/25/2008	10:20	42/34	7/3/1994	9:52	42/34
7/7/2007	10:27	42/34	7/16/1993	9:56	42/34
7/13/2006	10:20	41/34	7/29/1992	9:56	42/34
7/1/2005	10:21	42/34	7/27/1991	9:57	42/34
7/30/2004	10:16	42/34	7/8/1990	9:53	42/34
7/12/2003	10:10	42/34	7/5/1989	9:34	42/34
7/25/2002	10:09	42/34	7/2/1988	10:04	42/34
7/22/2001	10:14	42/34	7/25/1987	9:52	41/34
7/19/2000	10:10	42/34	7/13/1986	9:56	42/34
7/17/1999	10:11	42/34	7/3/1985	9:57	41/34
7/30/1998	10:12	42/34	7/7/1984	10:02	42/34

The LEDAPS process uses average daily lamp brightness history to obtain calibration coefficients based on acquisition date. These calibration coefficients are used to determine the at-sensor radiance values (Masek et al., 2006). The LEDAPS process converts at-sensor radiance to top-of-atmosphere (TOA) by an algorithm that incorporates solar irradiance derived from the MODTRAN model, bandpass, earth sun distance and solar zenith angle (Masek et al., 2006).

The LEDAPS atmospheric correction assumes particle scattering and gaseous absorption can be decoupled (Masek et al., 2006). Surface reflectance is correlated with TOA reflectance using (1),

$$\rho_{TOA} = T_g(O_3, O_2, CO_2, NO_2, CH_4)\left[\rho_{R+A} + T_{R+A}T_g(H_2O)\frac{\rho_s}{1+S_{R+A}\rho_S}\right] \quad (1)$$

where ρ_s is the surface reflectance, T_g is the gaseous transmission, T_{R+A} is the Rayleigh and aerosol transmission, ρ_{R+A} is the Rayleigh and aerosol atmospheric intrinsic reflectance, and S_{R+A} is the Rayleigh and aerosol spherical albedo (Masek et al., 2006). The 6S radiative transfer model is used to derive surface reflectance from (1) with the input of aerosol optical thickness (AOT), atmospheric pressure and water vapor (Masek et al., 2006).

III. Methodology

This section describes the methods used to derive the DOS surface reflectance data set and the comparison tests performed.

A. *Simplified DOS Calculated Surface Reflectance Data*

Conversion of Digital Number (DN) to Top-of-Atmosphere Reflectance

The first step in analyzing raw Landsat data is converting the digital numbers to at sensor radiance values by removing the gain and offset caused by the sensors themselves (Chavez, 1996). Conversion of Calibrated Digital Number (Q_{cal}) to at sensor radiance is accomplished using (2),

$$L_\lambda = \left(\frac{L_{Max\lambda} - L_{Min\lambda}}{Q_{Cal\max}}\right) * Q_{cal} + L_{Min\lambda} \quad (2)$$

where L_λ = spectral radiance at the sensor's aperture in W/m^2•sr•μm (Chander and Markham, 2003). Conversion of Radiance (L_λ) to top-of-atmosphere (TOA) reflectance is accomplished using (3),

$$\rho_P = \frac{\pi \cdot L_\lambda \cdot d^2}{ESUN_\lambda \cdot COS\theta_s} \quad (3)$$

where ρ_P = unitless planetary reflectance, L_λ = spectral radiance at the sensor's aperture, d = earth sun distance in astronomical units, $ESUN_\lambda$ = mean solar exoatmospheric irradiances, θ_s = solar zenith angle in degrees (Chander and Markham, 2003).

Atmospheric Correction

An atmospheric correction is applied to obtain surface reflectance using a simple image based method called Dark Object Subtraction (DOS) which is based on the assumption that radiance seen at the satellite for "dark" pixels (i.e. deep water or shadow) result purely from atmospheric path radiance. This allows us to process imagery where atmospheric column data are not available (generally pre-2000). For this analysis DOS is performed using the Cos θ or "COST" technique developed by Chavez (1996). The first step in the DOS method is removal of a reflectance value representing the contribution of the atmospheric scattering effect from the DN recorded at the sensor. Two ways of selecting this value are the histogram approach in which the DN selected is the first below 1000 pixels for a typical Landsat image, or a simpler approach in which a known dark object is selected using the assumption that any DN from that pixel is the result of the atmospheric contribution.

Use of the histogram method typically requires analysis of the entire image (Chavez, 1988). Therefore, for this effort, the selection of the minimum pixel value representing the atmospheric haze was accomplished by selecting the minimum DN for each band over Black Lake. This mountain snowmelt fed water body is surrounded by trees and mountain shadow representing an ideal zero reflectance surface for the DOS method. The first step in the COST technique is to calculate the minimum radiance ($L_{\lambda, min}$) using (4),

$$L_{\lambda,\min} = L_{Min\lambda} + \left(\frac{L_{Max\lambda} - L_{Min\lambda}}{Q_{Cal\max}}\right). \quad (4)$$

Since no targets are completely black, even the dark object will contain some reflectance value. Therefore, the COST method assigns a 1% reflectance value to the selected dark object (Chavez, 1996). The theoretical radiance ($L_{\lambda, 1\%}$) of a dark object (assuming a 1% reflectance) is calculated using (5),

Proc. of the Intl. Conf. on Advances In Bio-Informatics,Bio-Technology And Environmental Engineering-ABBE 2014.

ISBN: 978-1-63248-009-5 doi: 10.15224/ 978-1-63248-009-5-87

$$L_{\lambda,1\%} = \frac{0.01 \cdot d^2 \cdot Cos^2\theta}{\pi \cdot ESUN_\lambda} \quad (5)$$

A haze correction factor ($L_{\lambda, haze}$) is then calculated using (6),

$$L_{\lambda,haze} = L_{Min\lambda} - L_{\lambda,1\%} \quad (6)$$

(Chavez, 1996). The corrected surface reflectance value (ρ_P) is then calculated using (7),

$$\rho_P = \frac{\pi \cdot d^2 \cdot (L_\lambda - L_{\lambda,haze})}{TAU_v \cdot ESUN_\lambda \cdot Cos\theta \cdot TAU_z} \quad (7)$$

where TAU_v represents the atmospheric transmittance from the ground to the sensor and TAU_z is the atmospheric transmittance from the sun to the ground. Since Landsat images are taken at a nadir angle, TAU_v is equal to Cos 0^o or 1.0. For the COST method, TAU_z is equal to the cosine of the solar zenith angle or Cos θ^o (Chavez, 1996). Therefore, the surface reflectance is calculated from (8) as:

$$\rho_P = \frac{\pi \cdot d^2 \cdot (L_\lambda - L_{\lambda,haze})}{ESUN_\lambda \cdot Cos^2\theta}. \quad (8)$$

B. *Comparison Methods*

Linear regression is used to determine the level of agreement between the two data sets. Surface reflectance values from each data set are plotted against each other and the regression statistics are calculated by the Excel statistical analysis tool. In this study, we consider the adjusted Coefficient of Determination (R^2) and the Standard Error (*SE*). The adjusted R^2 value is determined from the Pearson product correlation coefficient as shown in (9),

$$R = \frac{\sum (x-\bar{x})(y-\bar{y})}{\sqrt{\sum (x-\bar{x})^2 \cdot \sum (y-\bar{y})^2}} \quad (9)$$

where x and y are the sample means. The closer R^2 is to 1.0, the closer the data is to the more linear the relationship between the two variables. Adjusted R^2 value is then determined as shown in (10),

$$Adjusted\ R^2 = 1 - \frac{(1-R^2)\cdot(n-1)}{(n-k-1)} \quad (10)$$

where n is the number of observations and k is the number of predictors. The adjusted R^2 value is used in this study due to the large number of predictors which may artificially raise the true goodness of fit between the data sets if the unadjusted R^2 value is used.

The *SE* is the square root of the variance of the regression coefficient. It is a measure of how much variation exists in the data points about the regression line. It is another indicator of the general agreement between the variables with a smaller *SE* indicating closer agreement. The *SE* is calculated as shown in (11),

$$SE = \sqrt{\frac{1}{(n-2)}\left[\sum (y-\bar{y})^2 - \frac{\left[\sum (x-\bar{x})(y-\bar{y})\right]^2}{\sum (x-\bar{x})^2}\right]} \quad (11)$$

where n is the number of observations.

The results of the linear regression are examined for trends in the data over time. Trends in the data based on elevation gradient and vegetative density are also examined. Presence of trends in the correlation between the data sets may indicate a bias in the methodology used to derive the surface reflectance values. Trends are calculated using the non-parametric Mann-Kendall (MK) trend test. This analysis essentially determines if a set of values (y) are increasing or decreasing over time. Mann-Kendall analysis looks at the sums of the signs of the differences between successive data points and calculates a score or "S" statistic with the following properties: for S < 0 (values are decreasing over time); for S > 0 (values are increasing over time). The magnitude of the S-statistic is a measure of the strength of the trend. For a sample size of 28, S values of + or – 100 indicate a statistically significant trend with a p value of < 0.05. This means the null hypothesis of no-trend in the data can be discarded with the risk of committing a Type II (rejection of a true null or H_0) error at less than 5%. The MK S-statistic is calculated using (12),

$$S = \sum_{i=1}^{n-1} \sum_{j=i+1}^{n} sign\left(y_j - y_i\right) \quad (12)$$

where n is the number of observations and y_i (i = 1…n) is the value at time T_i and y_j (j = 1…n) is the value at time T_j (De Beurs and Henebry, 2005). These calculations are carried out in Excel using the XLSTAT add-in statistical application. This program generates the S statistic as well as the probability (p) value which is used to quantify the statistical significance of the trend. The p value is defined as the probability of obtaining a value of S equal or greater than the calculated value for n when no trend is present. The confidence factor (risk of rejecting a true null) is defined as (1-p)*100%.

IV. Results and Discussion

This section presents the results obtained from our comparison of the surface reflectance values published in the USGS CDR data set and those surface reflectance values calculated using the simplified DOS method using the COST approach.

A. *Comparison of all data sets*

This study examined the surface reflectance data for 105 sample sites for 28 dates. This provides a total of 2,940 individual data pairs in each of the six reflective bands of the Landsat 5 TM sensor. Fig. 2 shows the DOS and USGS derived data sets plotted against each other for each of the six reflective bands of the TM sensor. Table 4 summarizes the results of comparison between all the data pairs for each band.

Proc. of the Intl. Conf. on Advances In Bio-Informatics,Bio-Technology And Environmental Engineering-ABBE 2014.

ISBN: 978-1-63248-009-5 doi: 10.15224/ 978-1-63248-009-5-87

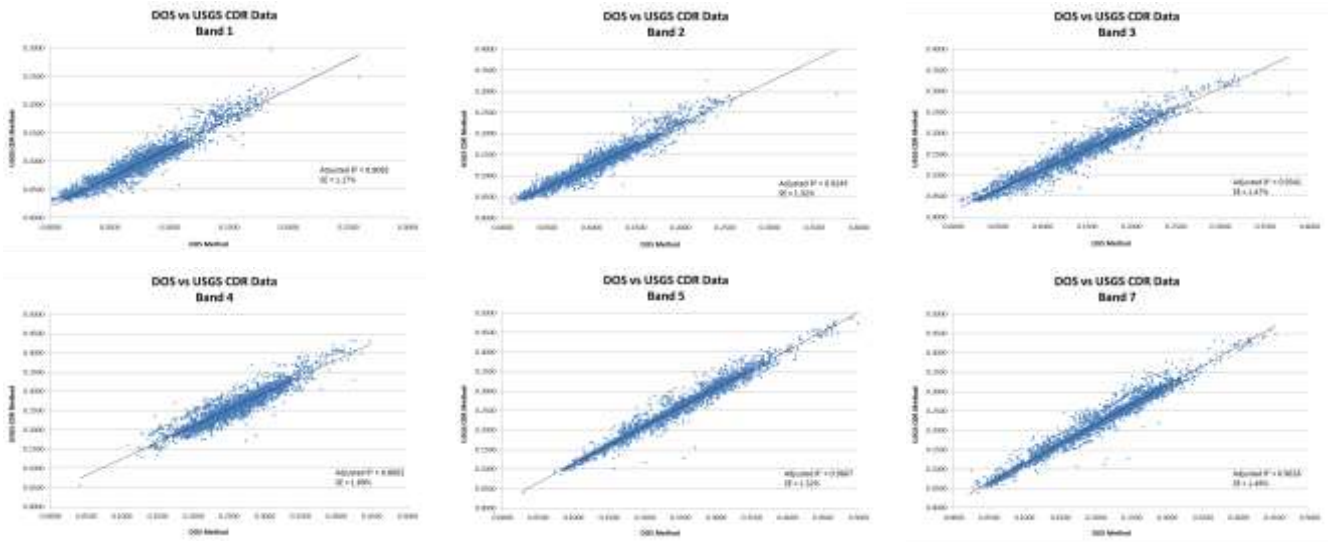

Figure 2: Comparison of surface reflectance values all 105 sample sites for Landsat 5 TM Bands 1, 2, 3, 4, 5, & 7.

TABLE 4: Adjusted R^2 and *SE* values for all data sets from 1984 through 2011

Adjusted R^2 Values						*SE* Values					
Band 1	Band 2	Band 3	Band 4	Band 5	Band 7	Band 1	Band 2	Band 3	Band 4	Band 5	Band 7
0.9082	0.9245	0.9341	0.8602	0.9667	0.9628	0.0117	0.0132	0.0147	0.0169	0.0132	0.0149

TABLE 5: Mean values and difference between the means for the surface reflectance value of each band

Band	Band 1		Band 2		Band 3		Band 4		Band 5		Band 7	
Method	DOS	USGS	DOS	USGS	DOS	USGS	DOS	USGS	DOS	USGS	DOS	USGS
Mean	0.078	0.100	0.111	0.133	0.136	0.148	0.257	0.259	0.248	0.256	0.198	0.213
Δ (%)	10.75		16.57		8.40		0.73		3.42		7.26	

Table 5 summarizes the means of the surface reflectance values by each method for each band and shows the difference in those mean reflectance values. We next provide a brief summary of the results of our comparison for each band.

For band 1, an adjusted R^2 value of 0.9082 combined with a SE of only 1.17% suggests very strong agreement between the two methods. The mean value of the USGS data set is approximately 10% higher than the DOS derived reflectance mean value for band 1. This suggests the DOS technique is over estimating the atmospheric contribution to the at-sensor radiance measurement for the band 1 region (0.45 – 0.52 μm).

Similar results are seen in bands 2, 3, 5, and 7 with very strong agreement in surface reflectance values derived by each method. Band 4 had the lowest agreement between the two methods. However, with an adjusted R^2 value of 0.8602 combined with a SE of only 1.69% strong agreement exists between the two methods in this region also.

B. Comparison of data sets over time

We next looked at the influence time has had on the different methods of deriving surface reflectance. Table 6 shows the trends in the adjusted R^2 and *SE* values for 105 sample sites in each band over the 28 year period from 1984 through 2011. Trends in the adjusted R^2 values are statistically significant in each band except band 5. Band 5 was strongly correlated throughout the 28 years study period, and the trend is also positive for this region of the spectrum.

This finding demonstrates that the agreement between the two methods has increased significantly over the time period of the study. This suggests that there is a difference in how the DOS and USGS methods accounted for variables such as sensor gain and offset. Several corrections to these values have taken place over the 28 year time span of this study. However, even though the agreement between the two methods has increased, the agreement in the early years of the study also showed R^2 values or 0.9 or better. The variation in how the DOS and USGS methods calculate surface reflectance values are not sufficient to produce tangibly different results.

Proc. of the Intl. Conf. on Advances In Bio-Informatics,Bio-Technology And Environmental Engineering-ABBE 2014.

ISBN: 978-1-63248-009-5 doi: 10.15224/ 978-1-63248-009-5-87

TABLE 6: Trends in adjusted R^2 and values for all data sets from 1984 through 2011

Trend	Band 1	Band 2	Band 3	Band 4	Band 5	Band 7
S	196	205	183	144	65	101
p	<0.0001	<0.0001	0.0003	0.004	0.206	0.048

C. *Comparison of data sets by Land Class*

Table 7 shows the results of the comparison between the USGS data set and the DOS derived surface reflectance for each of the top ten land cover classes present in the study area. There are 30 sample sites (3 for each land cover class), for each of the 28 years of the study providing a total of 840 data pairs for each band in this analysis.

The results of this analysis shows that the correlation between the USGS data sets and the DOS methodology varies significantly based on land cover classification. While most of the data sets show good agreement, Land class 3215 (Sierra Nevada Cliff and Canyon) in particular shows poor correlation between the two methods for determining surface reflectance. This is especially true in Band 3 (Red) where there is significant scatter among the data points as shown in fig. 3.

Sierra Nevada Cliff and Canyon land cover consist of rocky barren areas located in the foothills and sub alpine areas of the Sierra Nevada's. Typically less than 10% of the surface contains any vegetative species. The geography consists of steep cliff faces, rock outcrops, canyon walls and some talus (SWReGAP 2003). This suggests that extreme topographic variation within individual pixels has an impact on the surface reflectance determinations between the two approaches.

TABLE 7: Trends in adjusted R^2 values for all data sets from 1984 through 2011

Land Class	Adjusted R^2 Values					
	Band 1	Band 2	Band 3	Band 4	Band 5	Band 7
3504	0.9347	0.9327	0.9357	0.8573	0.9449	0.9432
4514	0.8764	0.8909	0.9220	0.7876	0.8787	0.8811
5308	0.6546	0.7314	0.7840	0.5600	0.8308	0.8104
5706	0.8682	0.8200	0.6909	0.2662	0.6598	0.5966
4533	0.5951	0.6424	0.6320	0.5380	0.4558	0.4177
3215	0.6401	0.4533	0.1735	0.5629	0.8646	0.5224
5205	0.9518	0.9516	0.9309	0.8639	0.5513	0.7174
1201	0.8072	0.4984	0.4870	0.2896	0.8075	0.7814
4318	0.9482	0.9523	0.9511	0.8412	0.9653	0.9640
4608	0.7182	0.8090	0.8577	0.7614	0.7755	0.8819

D. *Comparison of data sets by Elevation Gradient*

Next, we examine the results of the comparison between the USGS data set and the DOS derived surface reflectance at each elevation from 1200 meters MSL to 3600 meters MSL. There are 84 pairs of data at each elevation, (3 sites x 28 years).

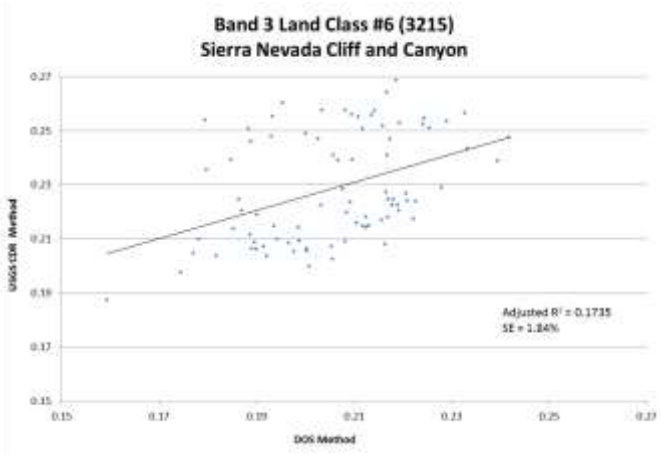

Figure 3: Comparison of surface reflectance values Sierra Nevada Cliff and Canyon Land Class for Landsat 5 TM Band 3 (RED 0.63 – 0.69 μm).

Table 8 shows that the correlation between the USGS data sets and the DOS methodology increase with elevation. Trends in the adjusted R^2 values in the SWIR and MWIR bands are not statistically significant and we can only infer that the USGS and DOS data sets show closer agreement at higher elevations from the positive S values. Although not statistically significant, the trends in the visible and NIR regions is strong suggesting closer agreement between the two surface reflectance methodologies at higher elevations.

E. *Comparison of data sets by Vegetative Density*

Table 9 shows the results of the comparison between the USGS data set and the DOS derived surface reflectance for densely, medium, and sparsely vegetated sites. There are 700 pairs of data for each vegetative density, (25 elevations x 28 years). This analysis indicates that the agreement between the USGS data and the DOS methodology declines with increasing vegetation density with the exception of band 7. Since the sparse areas have a higher absolute reflectance, the data shown here indicate correlation between the USGS data and the DOS data increases with absolute surface reflectance.

TABLE 8: Trends in adjusted R^2 and values for all data sets by elevation

Trend	Band 1	Band 2	Band 3	Band 4	Band 5	Band 7
S	90	86	47	90	8	2
p	0.037	0.047	0.283	0.037	0.870	0.982

TABLE 9: Adjusted R^2 values for densely, medium and sparsely vegetated sites

Density	Band 1	Band 2	Band 3	Band 4	Band 5	Band 7
Dense	0.7926	0.8507	0.8726	0.8356	0.9541	0.9394
Medium	0.8080	0.8664	0.8683	0.8745	0.9548	0.9335
Sparse	0.8853	0.8877	0.8931	0.9093	0.9770	0.9354

ISBN: 978-1-63248-009-5 doi: 10.15224/ 978-1-63248-009-5-87

This observation is consistent with the previous finding for trends in the agreement between the two methods based on elevation gradient since vegetation density tends to decline at higher elevation; we observe the R^2 value increase with elevation.

Confidence Levels

Multitemporal satellite imagery is impacted by several factors including changes in sensor response, sensor stability, atmospheric effects, and illumination effects (Vicente-Serrano et al., 2008). Radiometric uncertainty for the TM data is approximately 5% (Chander et al., 2009).

The USGS surface reflectance data set has been assessed against MODIS surface reflectance data and found to be highly correlated with discrepancies between 2.2 to 3.5 percent (Feng et al., 2013).

v. Summary and Conclusions

This study compared the surface reflectance values published in the USGS Climate Data Record archive with surface reflectance calculated using a simple Dark Object Subtraction method. The ecologically sensitive Big Pine Creek watershed served as the study site and 105 sample locations within that watershed were examined for 28 dates in each of the six reflective bands of the Landsat 5 TM imager. Simple linear regression was used to compare the surface reflectance values determined by each method. In addition to looking at a complete comparison of all the data pairs, sample sites were analyzed based on land cover class, elevation, and vegetative density. Trends in the data over time and by elevation were also determined.

The overall comparison of the two methods showed very close agreement in the surface reflectance values, with band 7 showing the closest agreement (adjusted R^2 = 0.9628) and band 4 shown the least (adjusted R^2 = 0.8602). Mean surface reflectance values from the USGS CDR data set are generally higher than the values determined by the DOS method with band 2 showing the highest difference between the means (16.57%) while band 4 showed the least difference between the means (0.73%). The statistically significant positive trends in the level of agreement between the two methodologies over time suggests differences in the values used for the gains and offset values for the Landsat 5 TM sensor. These values were revised periodically to correct for changes in the radiometric response of the sensor over time or for improved calibration data sets (Chander and Markham, 2003).

The greatest discrepancy between the two methodologies is found in comparisons of surface reflectance over the land class 3215 (Sierra Nevada Cliff and Canyon). This may be the result of the large topographical variations within individual pixels that can occur for this land cover class. While this one result makes it clear that discrepancies do exist in the two methodologies, the primary conclusion we draw from the results of this study is that the USGS derived CDR data base shows good agreement with the data generated using previous methods. This suggests that the need to revisit past studies using the newly available surface reflectance data set would not result in new findings or altered conclusions.

References

[1] N.D. Bowerman and D.H. Clark, "Holocene glaciation of the central Sierra Nevada, California," Quaternary Science Reviews Vol. 30, pp. 1067-1085, 2011.

[2] G. Chander and B. Markham, "Revised Landsat-5 TM radiometric calibration procedures and postcalibration dynamic ranges," IEEE Transactions on Geoscience and Remote Sensing, Vol. 41, No. 11, pp. 2674-2677, 2003.

[3] G. Chander, B. Markham, and D.L. Helder, "Summary of current radiometric calibration coefficients for Landsat MSS, TM, ETM+, and EO-1 ALI sensors," Remote Sensing of Environment, Vol. 113, pp. 893-903, 2009.

[4] P.S. Chavez, "An Improved Dark-Object Subtraction Technique for Atmospheric Scattering Correction of Multispectral Data," Remote Sensing of Environment, Vol. 24, pp. 459-479, 1988.

[5] P.S. Chavez, "Image-based atmospheric corrections–revisited and improved," Photogrammetric Engineering and Remote Sensing, Vol. 62, No. 9, pp. 1025-1036, 1996.

[6] D.J. Chmura, P.D. Anderson, G.T. Howe, C.A. Harrington, J.E. Halofsky, D.L. Peterson, D.C. Shaw, and B.J. St. Clair, "Forest responses to climate change in the northwestern United States: Ecophysiological foundations for adaptive management," Forest Ecology and Management, Vol. 261, pp. 1121–1142, 2011.

[7] S.Y. Chung, P. Ehrenfreund, J.D. Rummel, and N. Peter, "Synergies of earth science and space exploration," Advances in Space Research, Vol. 45, pp. 155–168, 2010.

[8] K.M. De Beurs and G.M. Henebry, "A statistical framework for the analysis of long image time series," International Journal of Remote Sensing, Vol. 26, No. 8, pp. 1551-1573, 2005.

[9] A.J. Elmore, J.F. Mustard, and S.J. Manning, "Regional patterns of plant community response to changes in water: Owens Valley, California," Ecological Applications, Vol. 13, No. 2, pp. 443-460, 2003.

[10] M. Feng, J.O. Sexton, C. Huang, J.G. Masek, E.F. Vermote, F. Gao, R. Narasimhan, S. Channan, R.E. Wolfe, and J.R. Townshend, "Global surface products from Landsat: Assessment using coincident MODIS observations," Remote Sensing of Environment, Vol. 134, pp. 276-293, 2013.

[11] V. Gond, D.G. De Pury, F. Veroustraete, and R. Cuelemans, R., "Seasonal variation in leaf area index, leaf chlorophyll and water content; scaling up to estimate fAPAR and carbon balance in a multilayer, multispecies temperate forest," Tree Physiology, Vol. 19, pp. 673-679, 1999.

[12] G.M. Kondolf, "Stream-groundwater interactions along streams of the Eastern Sierra Nevada California: Implications for assessing potential impacts of flow diversions," USDA Forest Service Gen. Tech. Rep. PSW-110, pp. 352 – 359, 1989.

[13] J.G. Masek, E.F. Vermote, N. Saleous, R. Wolfe, F.G. Hall, F. Huemmrich, F. Gao, J. Kutler, and T.K. Lim, "A Landsat surface reflectance data set for North America, 1990-2000," IEEE Geoscience and Remote Sensing Letters, Vol. 3, pp. 68-72, 2006.

[14] O. Skre and M. Naess, "CO_2 and winter temperature effects on white birch," Chemosphere: Global Change Science, Vol. 1, pp. 469-483, 1999.

[15] SWReGAP, "Southwest Regional Gap Analysis Project Land Cover Legend, Ecological Systems and Alliance Descriptions," The Nature Conservancy 1815 N. Lynn Street Arlington, Virginia 22209, 2003.

[16] W. Turner, S. Spector, N. Gardiner, M. Fladeland, E. Sterling, and M. Steininger, "Remote sensing for biodiversity science and conservation," Trends in Ecology and Evolution, Vol. 18, No. 6, pp. 306–314, 2003.

[17] USGS, "United States Geological Survey Landsat Climate Data Record (CDR) Surface Reflectance Version 2.0," US Department of Interior Product Guide, March 2013.

[18] S.M. Vicente-Serrano, F. Perez-Cabello, and T. Lasanta, "Assessment of radiometric correction techniques in analyzing vegetation variability and change using time series of Landsat imagery," Remote Sensing of Environment, Vol. 112, pp. 3916-3934, 2008.

Proc. of the Intl. Conf. on Advances In Bio-Informatics,Bio-Technology And Environmental Engineering-ABBE 2014.

ISBN: 978-1-63248-009-5 doi: 10.15224/ 978-1-63248-009-5-87

About Author (s):

"While discrepancies do exist in the two methodologies, the primary conclusion we draw is that the USGS derived CDR data set shows good agreement with the data generated using previous methods"

Patrick Sawyer received his B.S. degree in Chemical Engineering in 1989 from California State University, Long Beach and a M.S. in Environmental Science from the University of Nevada, Las Vegas (UNLV). He is currently in the Environmental Science PhD program at UNLV. His research focus is on the use of remote sensing imagery to identify the impacts recent climate change has had on alpine environments.

Mr. Sawyer is a Certified Hazardous Materials Manager. He manages a federal research facility as a contractor for the US Department of Energy. He has over 15 years' experience in the development and execution of high hazard experiments for the US government. Prior to his government contracting work, Mr. Sawyer spent several years as a chemical engineer for Bechtel Corporation on a variety of projects in the US. Mr. Sawyer is a member of the American Chemical Society, the American Institute of Chemical Engineers, and the Academy of Hazardous Materials Managers.

"The USGS surface reflectance climate data record opens up the field of remote sensing ecosystem analysis to researchers who once discarded such tools due to their computational complexity"

Dr. Haroon Stephen received his B.S. degree in Agricultural Engineering in 1995 from the University of Agriculture Faisalabad, Pakistan; an M.S. degree in Remote Sensing and GIS in 1997 from the Asian Institute of Technology, Bangkok, Thailand; and a Ph.D. degree in Electrical and Computer Engineering in 2006 from Brigham Young University, Provo, Utah. He joined UNLV Water Resources Lab in 2007 as a postdoctoral researcher. Currently, he is serving UNLV as Director of the GIS and Remote Sensing Core Lab.

Dr. Stephen has diverse research experience in the areas of Remote Sensing, GIS, and GPS applications. His Ph.D. research involved the modeling of microwave scattering and emission behavior of electromagnetic waves over Saharan sand surfaces and Amazon vegetation. His ongoing research interests include applications of remote sensing and GIS technologies to water resource mapping; drought study; and climate change study. Presently, he is involved in several Federal and State sponsored research projects involving geospatial data research and applications. He is also developing a geovisualization facility at UNLV that will provide state-of-the-art visualization for the research and educational needs of UNLV and the region.